

J. Staples, D. Oshatz, T. Saleh, LBNL, Berkeley, CA 94720, USA

### Abstract

The medium-energy beam transport (MEBT) of the Spallation Neutron Source (SNS) is described. It transports a 2.5 MeV, 52 mA  $H^-$  beam through a series of 14 quadrupoles and four 402.5 MHz rebuncher cavities from the RFQ to the DTL. A 10-nsec rise/falltime traveling wave chopper/antichopper is incorporated in the transport lattice. Special emphasis is given to emittance preservation, which requires an unusually compact mechanical design. Details of the beam dynamics and mechanical design will be given.

## 1 REQUIREMENTS

The SNS comprises a 1 GeV  $H^-$  linac injecting approximately 1000 turns into an accumulator ring, which then extracts  $2.1 \times 10^{14}$  protons in one turn and directs the 2 MW average power beam to a liquid mercury target, all at a 60 Hz rate. The 1 msec-long beam accelerated by the linac incorporates a 300 nsec gap with a 945 nsec period, the period of the revolution frequency in the accumulator ring, to allow the 200 nsec rise of the extraction kicker magnet without scraping circulating beam on the Lambertson extraction magnet. One major function of the MEBT is to incorporate a fast traveling-wave chopper to provide this time structure of the injected beam. The beam will be pre-chopped in the LEBT at 65 keV, and the MEBT chopper sharpens the edges and deepens the 295 nsec notch.

An  $H^-$  bucket ion source [1] provides a 65 keV beam that is matched with a two-lens electrostatic LEBT [2] into a 3.7 meter-long 402.5 MHz RFQ [3] and transported by the 3.6 meter-long MEBT to the first 7.5 MeV tank of a 86 MeV, 402.5 MHz DTL. The beam is subsequently accelerated to approximately 1 GeV by a 402.5 MHz side-coupled cavity linac followed by an 805 MHz superconducting structure. The beam must be matched from the RFQ into the chopper section of the MEBT, and then matched into the acceptance of the DTL. The traveling-wave chopper, supplied by LANL, has a risetime of less than 10 nsec.

In addition, diagnostic devices are supplied to monitor the beam quality during operation (run-time diagnostics) and to enable tuning of the MEBT itself (tuning diagnostics).

## 2 BEAM DYNAMICS

The physics design of the MEBT is tightly constrained by the requirement that the emittance growth be held to as low



Figure 1: MEBT Mechanical Layout

a value as possible. Emittance growth due to the nonlinear charge distribution of the beam requires that the focusing lattice be as regular as possible and that the focusing be strong. The rapid transverse phase advance in the RFQ (22 degrees per  $2\beta\lambda$  period) in the RFQ must be carefully matched into the two 62-cm drift lengths in the MEBT required to insert the 35-cm-long traveling-wave choppers, and the ensuing irregular lattice is what is primarily responsible for emittance growth.

To keep the emittance growth to under 20%, the beam from the RFQ is focused through a series of four quadrupoles at the beginning of the MEBT, quasi-adiabatically slowing the phase advance down from the RFQ and matching the beam into the first 62-cm section which includes the first traveling-wave chopper. Similarly, at the exit of the MEBT a series of four quadrupoles matches the beam into the first DTL tank. A 19.45 cm drift between the last MEBT quad and first DTL quad provides room for diagnostics and a gate valve, and the beam is at a double waist at the entrance of the DTL first quad, simplifying tuning.

Figure 2 shows the  $5\sigma$  beam envelope and the phase spread in the MEBT (1.5 cm and 90 degree full scales) in a Trace3D envelope simulation.

The central region of the MEBT comprises a symmetrical set of choppers (a chopper and an anti-chopper) and two sets of triplet quadrupoles. The 35 cm-long chopper deflects the 2.5 MeV  $H^-$  beam by 18 milliradians, and the first triplet focuses the deflected beam to a displaced trajectory 1.09 cm away from the undeflected closed orbit and parallel to it. At this point a target removes the deflected beam.

\* This research is sponsored by the Director, Office of Science, Office of Basic Energy Science, of the U.S. Department of Energy, Contract No. DE-AC03-76SF00098

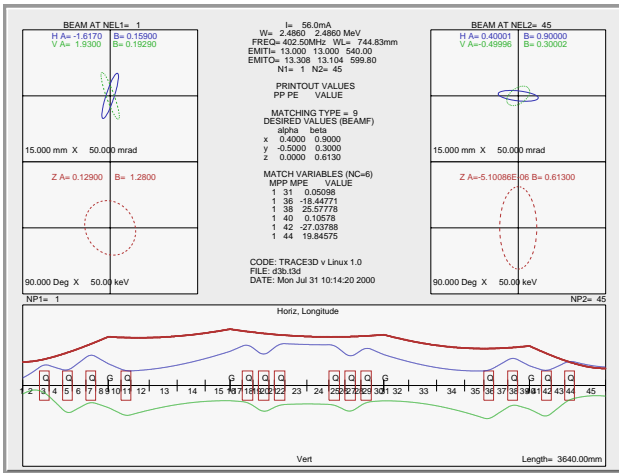


Figure 2:  $5\sigma$  Beam Envelope in MEBT

As the risetime of the chopper and its associated power supply may be as long as 10 nsec, some beam from as many as four r.f. micro-pulses may pass around the chopper target during the rise or fall of the chopper. These micro-pulses are returned to the beam axis by the symmetrical arrangement of a second quadrupole triplet following the chopper target and a traveling-wave anti-chopper operating in synchronism with the chopper (with a delay accounting for the transit time of the beam from the chopper to the antichopper). Any beam not intercepted by the target will be contained within the envelope of the unchopped beam. Simulations of beam through the linac show that an asymmetric beam distribution function from a partially chopped bunch does not excite instabilities which push the beam out of the undeflected beam boundary.

The beam on the chopper target is deflected vertically, and is wide in the horizontal plane, narrow in the vertical plane ( $\beta_x = 5$  meters,  $\beta_y = 1$  meter) resulting in a peak power density up to  $300 \text{ kW/cm}^2$ .

### 3 IMPLEMENTATION

The 3.6 meter-long MEBT incorporates 14 quadrupoles, four rebuncher cavities, two traveling-wave deflectors (choppers), a chopper beam stop and numerous diagnostics instruments.

The first and last four quadrupoles have a clear aperture diameter of 3.0 cm, and the middle six quadrupoles, where the beam is deflected by the choppers, 4.0 cm. Table 1 lists some quadrupole characteristics, with gradient, current and power for the highest excitation in each quadrupole series. The quadrupole design is derived from the LANL design used in APT [6].

Four 402.5 MHz rebuncher cavities focus the beam longitudinally to maintain the bunch structure and to match the beam optimally to the r.f. bucket of the 7.5 MeV DTL. As with the quadrupoles, the first and fourth cavities have a 3 cm beam aperture diameter, and the others a 3.6 cm aperture diameter. The peak integrated gradient  $\hat{V} = \int E_0 T dl$

Table 1: Quadrupole Specifications

	Small Bore	Large Bore	
Pole tip radius	3.2	4.2	cm
Peak Gradient	41	29	T/m
Effective Length	6.1	6.6	cm
Max Current	387	411	amps
Max Power	2928	3884	watts

varies between 45 and 106 keV. Table 2 lists the parameters of the rebuncher cavities.

Table 2: Cavity Specifications

	Small Bore	Large Bore	
Aper Diameter	3.0	3.6	cm
$\hat{V}$	75, 106	45, 50	keV
$Q_{\text{effective}}$	17400	17400	(80% $Q_0$ )
TTF	0.445	0.342	amps
Peak Power	11, 22	7, 8	kW

Two traveling-wave choppers, supplied by LANL [4], deflect the beam with a velocity  $\beta = 0.073$  by 18 mrad with a total potential of 4500 volts, balanced to ground, between the plates, which are spaced by 1.8 cm. The physical length is 35 cm, and the deflecting efficiency is about 90%.

The beam is initially chopped in the LEBT with a rise/falltime of less than 50 nsec [5]. The beam from the LEBT chopper is cleaned up and the edges sharpened by the MEBT chopper. The beam deflected onto the MEBT chopper target comprises two spikes, each less than 50 nsec long, for each of the approximately 1000 notches introduced in the 1 msec beam pulse.

The average power on the MEBT chopper target is less than 500 watts, but the peak power density in the core of the beam is  $300 \text{ kW/cm}^2$ . The design of a target that can withstand this high instantaneous power, even for short intervals, is a challenge. Furthermore, copper is ruled out as  $^{65}\text{Cu}$  has a neutron production threshold of 2.1 MeV for incident protons.

The target design utilizes a TZM (molybdenum alloyed with titanium and zirconium) front plate with 0.5 mm water-cooling microchannels and a 1 mm thickness between the water channels and the front plate. The beam hits the target at an angle of 75 degrees from the normal. The peak von Mises stress in the TZM is 65% of the yield stress, including a derating for fatigue failure. Figure 3 shows an outline view of the chopper target.

Several types of beam diagnostics are included. Figure 4 shows the diagnostics configuration. Due to the high peak power of the beam, intercepting diagnostics are not practical at full duty factor. The tuneup of the MEBT will be beam-based, with beam parameters established at critical points down the beam line that satisfy the tuning require-

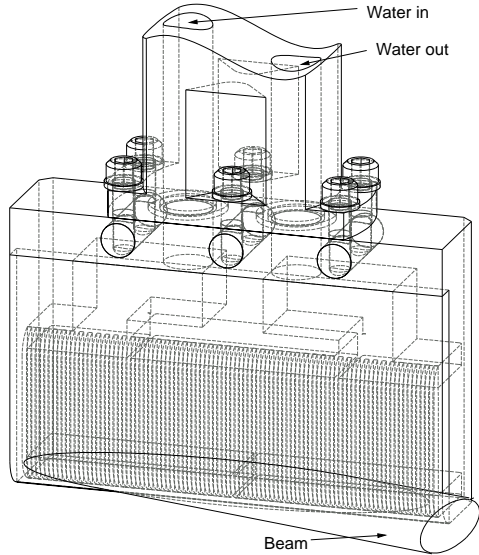


Figure 3: Chopper Target

ments.

Beam steering will be provided at six quadrupoles out of the fourteen, at places where the phase advance from one to the next in both transverse planes is about 90 degrees (with wide variation). These quads are the first and last units of the input matching section, of the output matching section, and of the six quadrupoles arranged around the chopper target. These quadrupoles also are the end quads in the three groups physically placed on three separate subrafts mounted on the MEBT girder.

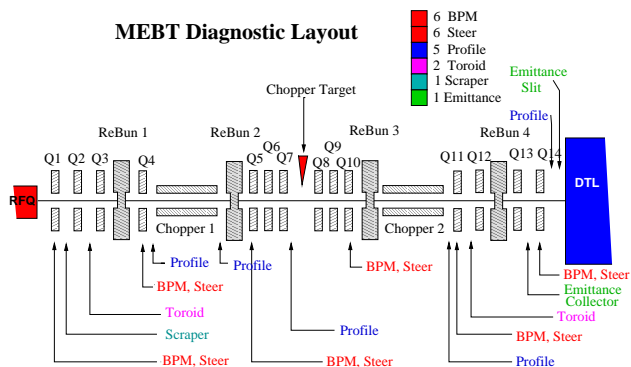


Figure 4: Diagnostics Layout

Backleg steering windings are added to the quadrupoles to produce a dipole field, steering up to 2 mrad. The sextupole component of the dipole field, due to the quadrupole symmetry of the iron, produces some emittance growth, but simulations show this to be less than 1% at full steering strength with random dipole phases.

Each of the six quadrupoles with steering windings also is fitted with a stripline beam position monitor (BPM). The second harmonic (805 MHz) induced wall current is analyzed with I and Q demodulator circuitry to determine both the centroid position of the beam and to extract phase in-

formation to tune the cavities using a TOF technique.

Five beam profile monitors are provided. Initially, traveling wires will be used at low duty factor, and we expect to implement residual gas background light monitors at a later date.

Two fast beam toroids are provided to measure the absolute beam current, one near each end of the MEBT. An active clamping system, synchronized to the chopper period, compensates for droop in the toroid response for the 1 msec long pulse.

The design of the MEBT vacuum system was driven by three factors: minimizing charge exchange beam loss, providing a reasonable vacuum at the interface with the DTL and pumping the hydrogen gas load from the chopper target. The maximum beam loss due to charge exchange in the MEBT is limited to less than 1%. Assuming a vacuum of  $1 \times 10^{-5}$  Torr (half hydrogen and half nitrogen equivalent) the beam loss would be 0.85%. The average vacuum along the beamline using the current design is expected to be in the mid  $1 \times 10^{-7}$  Torr range, this yields a loss of less than 0.1%. The MEBT will be pumped using 8 VacIon 55 liter/sec StarCell ion pumps, which pump hydrogen well. The system will be roughed down using two roughing vacuum carts consisting of a 550 liter/sec turbo-pump backed with a 300 liter/sec TriScroll pump. The system should rough down from atmospheric pressure to  $1 \times 10^{-5}$  Torr in approximately two hours, at which point the ion pumps can be turned on. The predicted vacuum at the MEBT/DTL interface is  $5 \times 10^{-7}$  Torr.

Magnets, rebuncher cavities and beamboxes are bolted and shimmed to individual rafts prior to installation of the rafts on the MEBT frame. Each of the three rafts is kinematically supported with a six-strut alignment system. Flexible vacuum bellows allow each raft to be aligned independently.

## 4 REFERENCES

- [1] R. Thomae, P. Bach, R. Gough, J. Greer, R. Keller, and K. Leung, Measurements on the H- Ion Source and Low Energy Beam Transport Section for the SNS Front-End Systems, this conference.
- [2] J. Reijonen, R. Thomae, and R. Keller, Evolution of the LEBT Layout for SNS, this conference.
- [3] A. Ratti, R. A. Gough, M. Hoff, R. Keller, K. Kennedy, R. MacGill, J. Staples, S. Virostek, R. Yourd, Fabrication and Testing of the First Module of the SNS RFQ, this conference.
- [4] S. Kurennoy, J. Power, D. Schrage, Meander-Line Current Structure for SNS Fast Beam Chopper, PAC99, p. 1399, New York
- [5] J. Staples, M. Hoff and C.F. Chan, All-Electrostatic Split LEBT Test Results, 1996 Linac Conference, Geneva, p. 157
- [6] A. Harvey, E. Hubbard, M. Schulze, S. Sheynin, D. Barlow, T. Hunter, Designs of the Low Energy Intertank Quadrupole Magnets for APT, PAC99, New York, p. 3576